

Reduction of increment of Rayleigh-Taylor instability in specially designed multilayer inertial-confinement-fusion targets

N. A. Inogamov*

Laboratoire de Physique Théorique de l'Ecole Normale Supérieure,† 24 rue Lhomond, 75231 Paris Cedex 05, France

(Received 30 December 1996)

The problem of hydrodynamic stability and mixing is very important for inertial-confinement-fusion (ICF) systems based upon high compression of fuel before ignition. The ablative drive of foils and compression of shells are unstable. The fundamental isobaric f^- mode is the most destructive one. It conserves pressures in the Lagrangian particles. A way to remove this dangerous mode is presented, based on special distributions of mass among subshells in the multishell target. The obtained solution follows from a consideration of new, inverse-density polytropes that have *negative* values of the polytropic index N , $\rho(r) \propto (r - r_V)^N$, where r_V is the radius of an inner, low-pressure cavity filled with a fuel. Polytropes describe inhomogeneous incompressible and compressible cases. Density of material ρ does not vanish in these distributions, as in the case of usual polytropes with $N > 0$ considered previously in geophysics and astrophysics. Conversely ρ rises when we approach the boundary with vacuum. This property allows us to simulate multilayer distributions of ρ that are typical for ICF targets. In these targets the high-density subshells surround the low pressure or vacuum cavity, while the outer subshells are made from low-density materials such as plastics, foams, and/or from composite materials. The proposed distributions are self-similar. Therefore their linear dynamics is scale invariant. New *acoustic* fundamental modes f_P^\pm are found and an interesting correspondence between acoustic and gravity modes is presented. (The f^\pm or f_G^\pm fundamental modes are the well-known gravity modes.) [S1063-651X(97)06810-4]

PACS number(s): 52.35.-g

INTRODUCTION

The program of laser inertial-confinement fusion has been developed over more than 20 years [1–4]. Powerful laser systems changed significantly during this time. The technology of target fabrication has also improved. To achieve high compression, the driving laser impulse (duration, shape) and the target structure must be mutually adjusted. Modern methods of fabrication [5–8] allow the preparation of smooth high quality targets with theoretically any desirable density profile $\rho(r)$. (Targets with several layers were widely used [5–8]. Technologically there is not a large difference between a deposition of one layer on another and a deposition of many layers.) This is done by coating with films of a wide variety of different materials and adjusting the thicknesses of these films. We propose the use of this technology to fabricate optimized profiles $\rho(r)$ with reduced increment of the instability. It is well known [3,4,9,10] that the Rayleigh-Taylor or interchange instability is the main obstacle to achieving the ignition threshold.

The optimal target is a set of subshells with densities ρ_i and thicknesses d_i , $1 < i < I$ (see Fig. 1). Here density ρ decreases and thicknesses increase in some definite way with radius r . The number I is large ($I \gg 1$); therefore relative jumps of density are small $2|\rho_{i+1} - \rho_i|/(\rho_{i+1} + \rho_i) \ll 1$.

These targets are thin and thick at the same time, since, from the one side, a thickness of the external coat d_I and the target as whole are large and, from the other side, high-density internal subshells are very thin. This means that an effective aspect ratio $R_{\text{eff}}/\Delta R_{\text{eff}}$ is intermediate between large ~ 100 and small ~ 1 values.

The isobaric Rayleigh-Taylor (RT) mode plays an important role in the theory of the instability. This mode satisfies the incompressibility condition $\text{div} v = 0$. Therefore pressures in Lagrangian particles are conserved during motion. The mode satisfies the isobaric boundary condition, which means that pressure is constant at a contact (Lagrangian) surface. It has the maximum increment $\sigma = \sqrt{gk}$ among all possible unstable modes. The mode is invariant to profiles of stratification and to equations of state (EOS), which may be different in different layers or Lagrangian particles. It is connected closely with isobaric gravity and trochoidal waves [11] and cannot not be eliminated by changes to the profile.

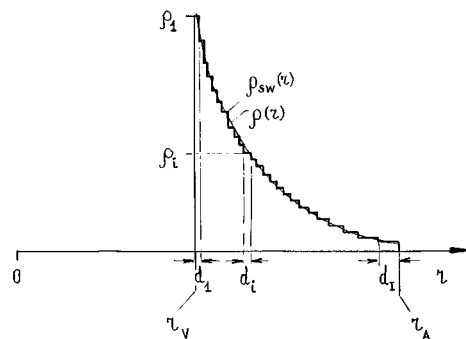


FIG. 1. Typical decreasing distributions of density $\rho_{sw}(r)$ in the multilayer targets.

*Permanent address: Landau Institute for Theoretical Physics, 142432, Moscow region, Chernogolovka. Electronic address: nail@landau.ac.ru

†Unité propre du CNRS, associée à l'Ecole Normale Supérieure et à l'Université de Paris Sud.

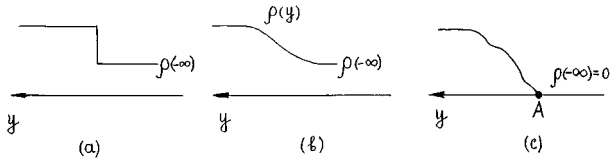


FIG. 2. The inefficiency of the usual profiling and smoothing in the important case of the ablating front when the density strongly decreases. The y axis is directed opposite the acceleration of gravity.

An interesting proposal of profiling in the case of an incompressible fluid [12] was to smooth out the step, as illustrated in Figs. 2(a) and 2(b). In the case of the step an increment $\sigma = \sqrt{Agk}$, $A = (1 - \mu)/(1 + \mu)$, $\mu = \rho_D/\rho_U$, $\rho_D = \rho(-\infty)$, $\rho_U = \rho(\infty)$ is unbounded. This means that at short wavelengths the instability is very fast ($\sigma \rightarrow \infty$ as $k \rightarrow \infty$). In the smoothed case this unbounded increment is ‘‘cut’’ or limited at large k by the Brunt-Väisälä increment $\sigma_{BV} = \sqrt{gd \ln \rho_0 / dy}$. Here 0 indicates an equilibrium distribution. We have put the maximum value of the derivative as $d \ln \rho_0 / dy$. In the compressible case we have

$$\begin{aligned} \sigma_{BV}^2 &= \frac{g}{\gamma} \left(\frac{-d \ln s_0}{dy} \right) = g \left(\frac{g}{c_0^2} + \frac{d \ln \rho_0}{dy} \right) \\ &= -g\beta[\nabla T - (\nabla T)_{AD}], \\ \beta &= - \left(\frac{\partial \ln \rho}{\partial T} \right)_p, \quad (\nabla T)_{AD} = - \frac{\beta g T}{c_P}, \\ \gamma &= \frac{c_P}{c_V} = \frac{n_F + 2}{n_F}, \quad m c_P = \frac{\gamma}{\gamma - 1}, \end{aligned}$$

where s_0 is a distribution of entropy, γ is an adiabatic exponent, c_P and c_V are heat capacities at constant pressure and volume, respectively, n_F is the number of degrees of freedom of a molecule, β is the coefficient of heat expansion, and $(\nabla T)_{AD}$ is the adiabatic gradient. For an ideal gas $p = \rho T/m$ we have $\beta = 1/T$, where m is the molecular weight. In astrophysical applications the frequency $\sqrt{-\sigma_{BV}^2}$ is usually denoted by the symbol N . Local values of functions σ_{BV} or ω_{BV} are used in well-known WKB asymptotics.

This ‘‘cutting’’ of an increment at $k \rightarrow \infty$ by the smoothing of the step leads to a delay $\sim 1/\sigma_{BV}$ in a turbulent mixing of the smoothed profile in comparison with mixing of the step. This has been clearly demonstrated recently by numerical simulation [13]. For large scales Y , $Y(\rho_0)_y/\rho_0 \gg 1$, and late times T , $T\sigma_{BV} \gg 1$, the smoothing and this delay are unessential. But at early and intermediate times they may be very valuable.

It is important that the density at the lower limit is not very small $\rho(-\infty) \neq 0$. The smoothing is inefficient for the case shown in Fig. 2(c). In this case the boundary condition at point A becomes isobaric and the isobaric RT mode appears in the spectrum. We have $\sigma_{BV} \rightarrow \infty$ at $\mu \rightarrow 0$ for this particular case. If the distribution $\rho(y)$ near the lower boundary with the homogeneous region may be fitted by the power law (index PL) function

$$\begin{aligned} \rho(y) &= \mu \rho_U \left(\frac{y - y_{PL}}{\epsilon} \right)^N, \quad y > y_{PL} + \epsilon, \\ \rho(y) &= \mu \rho_U, \quad y < y_{PL} + \epsilon, \end{aligned}$$

then the maximum value of the local increment is $\sigma_{BV} = \sqrt{gN/\epsilon}$, $\epsilon/d \approx \mu^{1/N}$, where d is the thickness of the smoothed layer. In the case of $\mu \approx 1$ the maximal increment σ_{BV} is $\sqrt{d/\epsilon}$ times smaller.

The situation for very small μ is interesting for fusion applications, since the boundary condition at the ablating front in the case of dangerous long-wavelength perturbations $k = k_A < a^2 g / 4b^2 v_A^2 = (a^2 / 4b^2) M_A^{-2} / h$, $h = c^2 / g$ may be approximated by the isobaric boundary condition; here v_A is a velocity of the ablating front in a cold plasma, and c is the velocity of sound in this plasma. This means that the increment of these perturbations is approximately the same as the classical one. The estimate of k_A follows from the well-known [14] Takabe formula $\sigma_A = a \sqrt{gk} - b k v_A$, with $a \approx 0.9$, $b \approx 3$; Mach number $M_A = v_A / c$ of the front is small: $M_A \ll 1$. A similar estimate also follows from an expression for σ_A given in Ref. [15].

It should also be mentioned that the dynamics of an internal region remote from the ablating front is important independently of the situation at the front. For example, such remote instabilities have been studied recently in experiments [16].

It seems necessary to expand Cowling classification used in astrophysics [17,18]. These are p , g^\pm , and f modes. There are pressure or sonic waves (p modes), stable gravity (g^+ , $\omega^2 > 0$), and unstable (g^- , $\omega^2 < 0$) modes, and one fundamental f mode. A naturally expanded classification includes

$$p, \quad g^+, \quad g^-, \quad f^+, \quad f^-$$

modes. [Below in Sec. VI it will be shown that, in addition to the f^\pm gravity modes, acoustic modes that are invariant (fundamental means invariant) to a stratified profile exist.] The mode f is now an f^+ mode. Isobaric properties of this classical mode are well known (see works by Gerstner and Rankin cited in Ref. [11]). The isobaric RT mode will be called the fundamental f^- mode.

We do not propose to eliminate the f^- mode from the spectrum by the profile shown in Fig. 1. This is impossible. Instead, we intend to remove it far from the important internal region at the expense of the large thicknesses of the outer subshells. There are low-density subshells. Therefore the gradient $|\nabla p|$ is small in this outer region and the ablative pressure p_A effectively accelerates the dense internal subshells.

The important region is the region near the internal boundary r_V or $y_V = 0$. The large-density subshells are here. They are most important for the compression process. The reason for the space separation of the f^- and g^- modes is as follows. In the proposed optimal profiles the gradient $|\nabla \rho|$ rises when we approach the r_V boundary. The g^- modes are in the region of maximum gradients. They are in the layer with thickness $\sim 1/k$ near the r_V boundary, as shown in Fig. 3. The f^- mode decays exponentially at the length $1/k$ in the direction away from the ablating front. The decay of the g^-

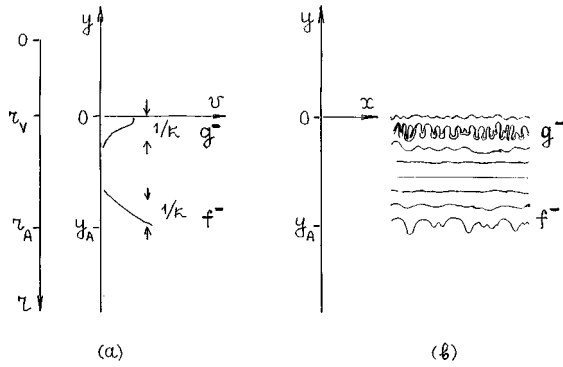


FIG. 3. The separation of the unstable region connected with the f^- mode and the appearance of two unstable regions and two mixing zones connected with the f^- and g^- modes, respectively, in the case of the proposed multilayer target.

and f^- modes is shown in Fig. 3(a). Therefore, two different separated regions of instability and mixing appear near the boundaries r_V and r_A (or $y_V=0$ and y_A); see Fig. 3. In Fig. 3(b) isodensity contours are shown.

The instability caused by the f^- mode cannot be changed. The increment of this mode is fixed and we cannot reduce it. The increment in the case of the g^- mode depends on the stratification of the profile, and may be reduced.

The optimal profiles are self-similar polytropes described by power-law functions. For example, the density profile is $\rho \propto (-y)^N$, with N the polytropic index. The self-similarity condition means that dimensional parameters are absent. Therefore the spectral theory is scale invariant. The expression for the increment is $\sigma_m = \sqrt{\Sigma_m g k}$, where Σ_m are dimensionless functions, and the index m denotes the denumerable set $\{m\}$ of discrete eigenvalues. In the qualitative sense the expression for σ is the same as in the simple case of the jump in an incompressible fluid. In the unstable case the mode with the largest increment is interesting. Usually it corresponds to the ‘‘ground’’ state with $m=0$.

We also mention that the dependence of Σ_0 ($\Sigma_0 = \sigma_0^2/gk$) on the variable parameter N may be used for the optimization. The increase of N improves the one-dimensional performance of targets. It decreases the value of energy necessary for the ignition. But, on the other hand, this leads to an intensification of instability. Therefore, some intermediate value must exist that corresponds to a reduced threshold of the ignition. This may be valuable when this threshold is not achieved. It also seems attractive because only improvements in target design are used instead of an expensive amplification of laser energetics.

The polytropes studied here have negative index N . Therefore $\rho \rightarrow \infty$ as $y \rightarrow 0$. In the usual polytropes studied in connection with geophysical and astrophysical applications [19–22], we have $N > 0$ and $\rho \rightarrow 0$ as $y \rightarrow 0$. The comparison of these cases is shown in Fig. 4. In both cases there is a low pressure region at $y > 0$. The acceleration of gravity is directed down in Figs. 4(a) and 4(b).

I. MAIN EQUATIONS

A system of equations following from mass, impulse, and energy conservation laws is

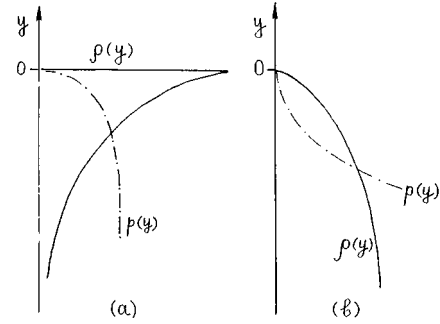


FIG. 4. The comparison of the inverse (a) and usual astrophysical (b) polytropes. Both have a boundary with vacuum $p(0)=0$. The distributions of pressure $p(y)$ are shown by dot-dashed curves. The acceleration of gravity is in the direction opposite to the y axis in both cases.

$$\begin{aligned} \rho_t + \text{div}(\rho v) &= 0, & \rho v_t + (v \nabla)v + \nabla p - \rho \vec{g} &= 0, \\ s_t + (v \nabla)s &= 0, & s &= s(p, \rho), \end{aligned}$$

where $s(p, \rho)$ is an arbitrary EOS and s is entropy. The energy equation is rewritten in the form $D_t p = c^2 D_t \rho$, where $D_t = \partial_t + (v \nabla)$, $c^2 = (\partial p / \partial \rho)_s$. The system is linearized in the usual way, $\propto e^{\sigma t + ikx}$, near the hydrostatic equilibrium [$\rho_0(y)$, $c_0(y)$, $dp_0(y)/dy = -g\rho_0(y)$]. An equation that links Lagrangian (p_L) and Eulerian (p_E) perturbations of pressure is added to the system. The final system is

$$\begin{aligned} \rho + \frac{k\rho'_0 v}{\sigma} &= \frac{p_L}{c_0^2}, & \frac{\rho_0 u}{ik} &= \frac{p_E}{-\sigma}, & v &= \frac{kp'_E + g\rho}{-\sigma\rho_0}, \\ \frac{p_E - p_L}{\rho_0} &= \frac{gv}{\sigma}, & \frac{-p_L}{\rho_0 c_0^2} &= \frac{iku + kv'}{\sigma}. \end{aligned}$$

Here the prime means differentiation on $\eta = ky$.

Perturbations of ρ and u are included algebraically, and perturbations of p_L and p_E are equivalent. After an algebraic elimination of unknown functions ρ , u , and p_E , we obtain a system of two equations for p_L and v . It is equivalent to the full linear system. This system is

$$\begin{aligned} v'_\eta + \frac{v}{\Sigma^2} &= - \left(1 + \frac{\sigma^2}{k^2 c^2} \right) \frac{k}{\sigma \rho} p_L, \\ \frac{v'_\eta}{\Sigma^2} + v &= - \frac{k}{\sigma \rho} \left[(p_L)_\eta' + \frac{g}{kc^2} p_L \right], \end{aligned} \tag{1.1}$$

where $\Sigma^2 = \sigma^2/gk$. We will omit the index 0 for unperturbed functions c and ρ , since the perturbations of these functions will not be used. If we exclude v from the system of equations (1.1), then we obtain the equation

$$(p_L)''_{\eta\eta} - \frac{(\rho)_\eta'}{\rho} (p_L)_\eta' - \left[1 - \frac{\rho'_\eta}{\Sigma^2 \rho} + \left(\Sigma^2 - \frac{1}{\Sigma^2} \right) \frac{g}{kc^2} \right] p_L = 0. \tag{1.2}$$

A similar equation usually written for an unknown function $\chi = \text{div } v$ is well known [19,20]. If we exclude p_L , then we obtain an equation for v . It is

$$\begin{aligned} v''_{\eta\eta} + \left[\frac{\rho'_\eta}{\rho} - \frac{\sigma^2}{\Delta} \frac{(c^2)'_\eta}{c^2} \right] v'_\eta - \left[1 - \frac{\rho'_\eta}{\Sigma^2 \rho} + \frac{gk}{\Delta} \frac{(c^2)'_\eta}{c^2} \right. \\ \left. + \left(\Sigma^2 - \frac{1}{\Sigma^2} \right) \frac{g}{kc^2} \right] v \\ = 0, \end{aligned} \quad (1.3)$$

where $\Delta = -\sigma^2 - k^2 c^2$. Equations (1.2) and (1.3) are valid for an arbitrary equation of state.

In the incompressible case the velocity of sound is large, and Eqs. (1.1) are

$$v'_\eta + \frac{v}{\Sigma^2} = -\frac{k}{\sigma} \frac{p_L}{\rho_0}, \quad \frac{v'_\eta}{\Sigma^2} + v = -\frac{k}{\sigma} \frac{(p_L)'_\eta}{\rho_0}. \quad (1.4)$$

Equations (1.2) and (1.3) in this case are

$$L_- p_L = 0, \quad L_+ v = 0,$$

$$L_\pm = \frac{d^2}{d\eta^2} \pm \frac{1}{\rho(\eta)} \frac{d\rho(\eta)}{d\eta} \frac{d}{d\eta} - 1 + \Sigma^{-2} \frac{1}{\rho(\eta)} \frac{d\rho(\eta)}{d\eta}. \quad (1.5)$$

The equation $L_+ v = 0$ is a classical Rayleigh equation. It describes the dynamics of perturbations in an inhomogeneous incompressible fluid.

If the determinant of the system of equations (1.1), $\det = \Sigma^{-4} - 1$, does not equal zero, then the system may be resolved for v and v' . The equation, which defines v , if functions $p_L(\eta)$ and $(p_L)'_\eta$ are known, is

$$v = \frac{k}{\sigma} (\Sigma^2 - \Sigma^{-2})^{-1} \frac{-(p_L)'_\eta \Sigma^2 + p_L}{\rho}. \quad (1.6)$$

The velocity of sound drops out of Eq. (1.6); therefore, it is the same in the compressible and incompressible cases.

II. THE WAY TO REDUCE THE INSTABILITY

Consider the polytropic distribution

$$\begin{aligned} \rho \propto (-y)^N, \quad p \propto (-y)^{N+1}, \quad c = \left(\frac{\gamma g(-y)}{N+1} \right)^{1/2}, \\ s \propto (-y)^\theta, \quad \theta = 1 - N(\gamma - 1). \end{aligned} \quad (2.1)$$

The hydrostatic functions (2.1) are substituted into Eq. (1.2). After that we obtain

$$\eta(p_L)''_{\eta\eta} - N(p_L)'_{\eta} - (\eta - 2a - N)p_L = 0, \quad (2.2)$$

$$a = -\frac{1}{2} \left(N - \frac{N+1}{\gamma} \Sigma^2 + \frac{\theta}{\gamma \Sigma^2} \right). \quad (2.3)$$

The substitution $p_L = e^{\eta u}$, $\eta = -z/2$ transforms Eq. (2.2) into an equation for the confluent hypergeometric function

$z u_{zz} + (-N - z)u_z - au = 0$ [23], and the change $p_L = \eta^{N/2} \psi$, $\eta = z/(2a + N)$ transforms Eq. (2.2) to the steady-state Schrödinger equation $\psi_{zz} - (-E + U)\psi = 0$ for a particle in the Coulomb potential with an orbital momentum $l = N/2$, an energy $E = -(2a + N)^{-2}$, and potential $U = -1/z + l(l+1)/z^2$.

We will consider the case when the upper and lower mixing zones are separated in space; see Fig. 3(a). Then, to describe the g^- perturbations located in the upper zone near the surface $y_V = 0$ the vanishing as $y \rightarrow -\infty$ solution of Eq. (2.2) will be necessary. It is expressed through the function U defined in Ref. [23]:

$$p_L = e^{\eta U}(a, -N, -2\eta), \quad (2.4)$$

$$\begin{aligned} M(a, b, z) = \sum_{j=0}^{\infty} \frac{a_j}{b_j} \frac{z^j}{j!}, \quad a_j = a(a+1) \cdots (a+j-1), \\ a_0 = 1, \end{aligned}$$

$$\begin{aligned} U = -\frac{\pi}{\sin N\pi} \left[\frac{M(a, -N, -2\eta)}{\Gamma(a+N+1)\Gamma(-N)} \right. \\ \left. - (-2\eta)^{N+1} \frac{M(a+N+1, N+2, -2\eta)}{\Gamma(a)\Gamma(N+2)} \right]. \end{aligned} \quad (2.5)$$

We now consider the condition at the upper boundary. If it is the isobaric boundary, then its velocity and displacement are not zero and the function p_L equals zero on the boundary. Consider the simpler case first. In this case, we neglect the pressure inside the internal cavity $p_0(y_V) = 0$ and $y_V = 0$. The index N must be bound, $N > -1$, for the convergence of mass $\int \rho dy$ as $|y| \rightarrow 0$. We eliminate the first term in expression (2.5) for U to satisfy the condition $p_L(0) = 0$. It is necessary to hit into one of the poles $z_m = -m$, $m = 0, 1, 2, \dots$ of the function $\Gamma(z)$ which is a part of the denominator of the first fraction. Therefore, we have $a_m + N + 1 = -m$. It is easy to obtain the dispersion relation from this condition and the definition of a in Eq. (2.3). We omit branches corresponding to p and f^+ modes. The g^+ modes are absent. The fastest of the g^- modes has $m = 0$. Its increment is $\Sigma_0^2 = \sqrt{\beta^2 + \theta/(N+1)} - \beta$, $\beta = \gamma(N+2)/2(N+1)$.

In the incompressible case, as $\gamma \rightarrow \infty$, this expression is simpler. The increment is $(\Sigma_0^2)_{\text{rigid}} = -N/(N+2)$. The compressibility increases the increment $\Delta(N, \gamma) = \Sigma_0^2 - (\Sigma_0^2)_{\text{rigid}} > 0$. The function $\Delta(N, \gamma)$ increases monotonically if we fix the index N and decrease γ . The decrease of γ means an increase in the compressibility. The maximum value $\Delta(N, 1)$ is achieved at $\gamma = 1$. The relative significance of the compressibility depends on N . When the index N decreases, then the gap

$$\begin{aligned} \Delta(N, 1) = (\Sigma_0^2)_{\text{soft}} - (\Sigma_0^2)_{\text{rigid}} \\ = \frac{N+2}{2(N+1)} \left[\left(1 + 4 \frac{N+1}{(N+2)^2} \right)^{1/2} - 1 \right] + \frac{N}{N+2} \end{aligned} \quad (2.6)$$

between soft ($\gamma = 1$) and rigid ($\gamma = \infty$) cases decreases. At $N = -1$ the gap equals zero. The increment σ decreases

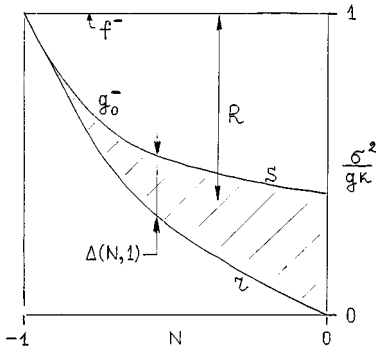


FIG. 5. The stabilizing influence of the polytropic profiling means that the increments are reduced by the shift R (where R is the reduction) in comparison with the case of the pure f^- mode. The increments are confined inside the dashed strip Δ .

when N rises at any fixed value of γ . It has a maximum at $N = -1$. The maximal increment equals \sqrt{gk} , as in the case of the f^- mode.

This is shown in Fig. 5. The expansion of Σ_0^2 in the maximum is

$$\Sigma_0^2 = 1 - 2\delta N + (2 + 4/\gamma)(\delta N)^2 + O[(\delta N)^3],$$

where $\delta N = N + 1$. We see that the linear term in δN is independent of γ . Therefore the expression $\Delta(N, 1)$ begins with the $(\delta N)^2$ term. The region $N < 0$, $\Sigma^2 > 0$ is the square bounded by limits at the upper and left sides. The upper limit is the increment $\sigma^2 = \sqrt{gk}$ of the f^- mode. The left limit is the condition $N > -1$. The reduced increments are inside the gap $\Delta(N, 1)$ defined by Eq. (2.6). The gap is dashed in Fig. 5. The curves r and s that bound the gap correspond to the rigid and soft cases, respectively. The polytropic increments are reduced in comparison with the increment of the f^- mode. The reduction is denoted by symbol R in Fig. 5. The stabilizing action of the profiling produces this reduction.

III. SHAPE OF EIGENFUNCTIONS

Consider the eigenfields of the problem. From expression (2.4) and the dispersion relation $a_0 = -N - 1$, the pressure in the case of the g_0^- mode is $p_L = (-\eta)^{1+N} e^\eta$, $\eta = ky$. The maximum of the function $p_L(\eta)$ is at $\eta_{pL}^{\max} = -1 - N$. The vertical velocity v is found from the p_L and Eq. (1.6). It equals

$$v = (1 - b^{-1}\eta)e^\eta, \quad -\eta_V^{\max} = 1 - b, \quad b = \frac{1 + N}{\Sigma_0^{-2} - 1} > 0. \quad (3.1)$$

The position of the maximum of the function v is given in Eq. (3.1). It appears to be located inside the polytrope. The proof of this is omitted because it is long.

The plots of the functions p_L and v are shown in Fig. 6. The maxima are asymmetric because the decay of the functions when we go away from the boundary is slower than their rise. If $N \rightarrow -1$, then the pressure p_L is a monotonic

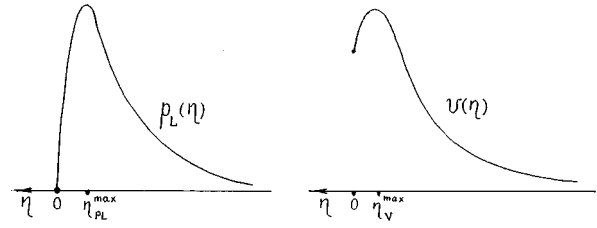


FIG. 6. The typical behavior of the eigenfunctions p_L and v . Velocity v remains finite at the vacuum boundary $y=0$. The perturbations are localized near the boundary.

function. It is necessary to emphasize the boundary behavior of the g^- modes. They decay as $e^{-k|y|}$ as $|y| \rightarrow \infty$. It is also interesting that the maxima of the perturbations are at some depth in spite of the fact that the maximum of the gradient $\nabla \rho$ is at the boundary.

The Taylor series for the maximum of velocity ($-\eta_V^{\max}$) near the end point $N = -1$ is

$$-\eta_V^{\max} = \frac{1}{2} + (1/2 - 1/\gamma)(\delta N) + (\delta N)^2/\gamma + O[(\delta N)^3].$$

In the incompressible case we have $(-\eta_V^{\max}) = 1 + N/2$. Consider the positions of the maxima of perturbations of Lagrangian pressure ($-\eta_{pL}^{\max}$) and velocity ($-\eta_V^{\max}$). It can be shown that there is a separation value N_{SEP} such that, for $-1 < N < N_{\text{SEP}}$, the maximum in velocity is beneath the maximum in pressure (that is, at a larger distance from the boundary), and vice versa for $N_{\text{SEP}} < N < 0$ (the pressure maximum is at a larger distance).

Consider the behavior of the eigenfunctions near the point $y=0$. It may be shown that (i) $p_L \rightarrow 0$ as $y \rightarrow 0$, (ii) velocity v is finite at the boundary, (iii) the ratio $v/c_0 \propto 1/\sqrt{-y}$ for $|y| \ll 1$, and (iv) a perturbation of Eulerian pressure $p_E = p_L + (g/i\omega)\rho_0 v \rightarrow \infty$ as $y \rightarrow 0$. The last circumstance is specific for the inverse density polytropes considered here. It differs from the astrophysical polytropes, for which density $\rho_0 \rightarrow 0$ as $y \rightarrow 0$ (see Fig. 4), and therefore we have $p_E \rightarrow 0$ as $y \rightarrow 0$.

The measure of the nonlinearity of the perturbation is the function $a(\eta) = p_L/p_0$. It defines the relative amplitude of the perturbations. The amplitudes of the velocity $v(0)$ and the relative pressure $a(0)$ are proportional ($v \propto a$, $|y| \ll 1$). If this ratio is small ($p_L \ll p_0$), the perturbations are linear. We have $p_L/p_0 \propto e^\eta$ for $m=0$. The maximum of the function $a(\eta)$ lies at the vacuum boundary $y=0$. It is important that this function remains bounded in the point $y=0$. From this it follows that, if $a(0) \ll 1$, the perturbations are linear everywhere.

This means that the singularities of the functions v/c_0 and p_E at the vacuum boundary are fictitious. Their presence does not mean that the perturbation of an arbitrary small amplitude at a large distance from the boundary will transfer into the nonlinear regime, and that shocks will appear near the vacuum boundary. Their appearance is due to a shift $\delta\eta$ in the perturbed boundary. In consequence of this the physical boundary is not at the point $y=0$. It is moved by the perturbation to the point $y=0 + \delta\eta$.

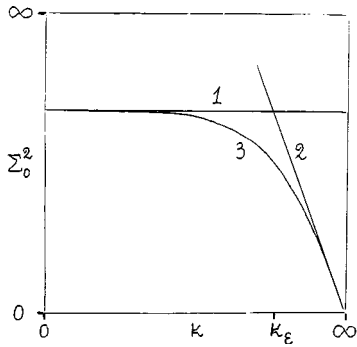


FIG. 7. The "cutting" or limiting of the spectrum in the case of the "cut" or limited power-law distribution.

In particular, in spite of the fact that formally the Mach number v/c_0 is large near the boundary, this means that the thin boundary layer is shifted as a whole. In this layer the local velocity of sound c_0 is smaller than $v(0)$. But accumulation of this velocity is a slow adiabatic process. It takes a long time in comparison with the time necessary for sound to pass this layer. This means that the acceleration due to the perturbation is small $|(\delta\eta)''| \ll g$. Therefore the gradients of pressure and the pressures themselves are small, $p_L \ll p_0$. From this it follows that the perturbation is linear.

IV. CASE OF NONZERO PRESSURE IN INTERNAL CAVITY

The answer will change if we consider the internal pressure. Let the pressure distribution be $p_L \propto (-y)^{N+1}$. The unperturbed boundary is at the point $y = y|_F = -\epsilon$. The value ϵ is defined by the pressure in the cavity p_ϵ ($\epsilon \propto p_\epsilon^{1/(N+1)}$).

In the case of the power-law distribution bounded by the pressure p_ϵ , the problem loses its self-similarity. Its spectrum is presented in Fig. 7. Here, line 1 corresponds to the self-similar (power-law) spectrum $\sigma_0 = \Sigma_0(N, \gamma) \sqrt{gk}$. The asymptotic curve 2 corresponds to the Brunt-Väisälä increment $\sigma_{BV} = \sqrt{g|s'_0|/\gamma s_0}$, which is evaluated at the edge of the profile at the point $y = -\epsilon$. It limits the growth of σ . The square of the dimensionless ratio is $\Sigma_{BV}^2 = (\theta/\gamma)/k\epsilon$, where θ has been defined in Eq. (2.1). The resulting dispersion curve is curve 3. It tends to the limiting curves 1 and 2 as $k \rightarrow 0$ and $k \rightarrow \infty$ respectively. The crossover region between these two asymptotes is $k \sim k_\epsilon = 1/\epsilon$.

At this stage of the acceleration of the shell the pressure in the cavity is small, $p_\epsilon \ll p_A$. Therefore, the shift ϵ is also small in comparison with the total thickness of the multilayer shell. In this case it is necessary to calculate the correction to the self-similar increment due to this counterpressure. This means that the parameter $k\epsilon$ is small, $k\epsilon \ll 1$. We find the first-order correction in the parameter $k\epsilon$ to the unperturbed increment $\sigma_0 = \Sigma_0 \sqrt{gk}$ (the index 0 means that the branch $m=0$ is considered).

The general dispersion curve, which is valid at the arbitrary value of the parameter $k\epsilon$, follows from the condition $p_L(-k\epsilon) = 0$. We use expression (2.4) for the solution

$p_L(\eta)$ and substitute it into this boundary condition. We then obtain the general relation

$$(2k\epsilon)^{N+1} \frac{\Gamma(-N)}{\Gamma(a)} - \frac{\Gamma(N+2)}{\Gamma(a+N+1)} \frac{M(a, -N, 2k\epsilon)}{M(a+N+1, N+2, 2k\epsilon)} = 0. \quad (4.1)$$

As $\epsilon \rightarrow 0$ the first term in relation (4.1) is eliminated, since $N > -1$ and the functions M tend to 1. In this case, studied in Sec. II, it is necessary to have the argument of the γ function at the pole $a+N+1 = -m$, $a = a_m$, $m = 0, 1, \dots$. Consider what will change at $\epsilon \neq 0$. If $k\epsilon \ll 1$, then the correction is small and we are near the pole. The asymptote $\Gamma(z) \approx [(-1)^m/m!]/(z+m)$, $m = 0, 1, \dots$ is valid in this vicinity. From this we obtain the required expression for the correction:

$$a_m = -m - N - 1 + \Delta a_m, \quad \Delta a_m = \frac{(-1)^m}{m!} \frac{\Gamma(-N)}{\Gamma(-m-N-1)\Gamma(N+2)} (2k\epsilon)^{N+1}. \quad (4.2)$$

It is interesting to note that the function $a_m(k)$ is the same for the sonic (p) and gravity (g^\pm) modes. From this it follows that their eigenfunctions p_L coincide at any value of ϵ . This is so because Eq. (2.4) includes the functions a , which are the same, and does not include the frequencies, which of course differ. All other functions (v , ρ , and so on) of the p and g^\pm modes differ because their definitions include frequencies.

We next analyze the obtained expressions. The function $\Gamma(x)$ at the real values of $x < 1$ alternates unit positive and negative intervals. From this it follows that at any value of $N > -1$ the corrections Δa_m , Eq. (4.2), are negative. If we substitute Eq. (4.2) into relation (2.3), which links a and σ , we obtain the biquadratic equation for σ . The negative root for this equation gives frequencies ($\sigma^2 = -\omega^2$) of the sonic waves. The positive root gives increments of the gravity modes. It follows from consideration of these roots that, due to the counterpressure p_ϵ , the p modes become harder and stable and the unstable g modes become softer. Therefore, curve 3 in Fig. 7 bends down from line 1 as k increases.

V. CASE OF RIGID BOUNDARY

We analyze another interesting modification by considering the change in the upper boundary condition. Consider the condition that is inverse to the free boundary condition. Let there be a rigid wall at the point $y = -\epsilon$.

The solution $p_L(\eta)$ of Eq. (2.1) that satisfies the lower boundary condition is given by Eq. (2.4). To find the spectrum it is necessary to satisfy the condition at the wall, $v(-k\epsilon) = 0$. This condition, together with Eq. (1.6), gives the dispersion relation $[(p_L)'_{\eta} \Sigma^2 - p_L]_{(-k\epsilon)} = 0$. Here substitute Eqs. (2.4) and (2.5) and differentiate. We obtain

$$\begin{aligned}
& -\frac{1-\Sigma^{-2}}{2} \frac{M(a, -N, 2k\varepsilon)}{\Gamma(a+N+1)\Gamma(-N)} + (2k\varepsilon)^{N+1} \frac{1-\Sigma^{-2}}{2} \frac{M(a+N+1, N+2, 2k\varepsilon)}{\Gamma(a)\Gamma(N+2)} - \frac{a}{N} \frac{M(a+1, -N+1, 2k\varepsilon)}{\Gamma(a+N+1)\Gamma(-N)} - (N+1) \\
& \times (2k\varepsilon)^N \frac{M(a+N+1, N+2, 2k\varepsilon)}{\Gamma(a)\Gamma(N+2)} - (2k\varepsilon)^{N+1} \frac{a+N+1}{N+2} \frac{M(a+N+2, N+3, 2k\varepsilon)}{\Gamma(a)\Gamma(N+2)} = 0. \tag{5.1}
\end{aligned}$$

Consider long wavelengths $k\varepsilon \ll 1$ first. If $N > 0$, then to zero order in $k\varepsilon$ the answer is the same as obtained above. The spectrum is given by relation $a_m + N + 1 = -m$. The first-order correction in $k\varepsilon$ is

$$\begin{aligned}
\Delta a_m &= \frac{(-1)^m}{m!} \left(-\frac{1-\Sigma_m^{-2}}{2} + \frac{N+1+m}{N} \right)^{-1} \\
& \times \frac{(N+1)\Gamma(-N)}{\Gamma(-N-1-m)\Gamma(N+2)} (2k\varepsilon)^N.
\end{aligned}$$

We see that the degree of the parameter $k\varepsilon$ has changed, compared with Eq. (4.2).

If $-1 < N < 0$, then the answer changes at the zeroth order in comparison with the case of the isobaric boundary described in Sec. II. In this case, it is necessary to eliminate the large fourth term in Eq. (5.1). To eliminate the term it is necessary to be at the pole of another gamma function $\Gamma(a)$. From this we obtain $a_m = -m$, $m = 0, 1, \dots$. To define Σ we have to substitute formula (2.3) for a in this equation. The solution of the equation is $\Sigma_m^2 = -\beta + \sqrt{\beta^2 + \theta/(N+1)}$, where $\beta = (\gamma/2)(2m-N)/(N+1)$. It is necessary to find the largest increments. Therefore we have to consider first the values of the index m .

At $m=0$ the expression under the root is the exact square. From this it follows that the answer in the case of m is $\Sigma^2 \equiv 1$ at any values of the indices N ($-1 < N < 0$) and γ . This is the indication to consider the case $\Sigma^2 = 1$ more carefully. It follows from the fact that in this case the system (1.1) degenerates and Eq. (1.6) becomes indeterminate because it includes the ratio $0/0$. This consideration is interesting and results in some significant general conclusions that will be better described in Sec. VI. Here we note that the dispersion relation $\sigma_0^2 = gk$ (the zero means that $m=0$) coincides with the relation for the isobaric f^- mode. At the same time the corresponding distribution $(p_L)_0$ is nonisobaric. In addition, if the f^- mode is a gravity mode then the mode discussed here is an acoustic one.

It follows from this study that the case $m=0$ must be omitted because of the violation of the boundary conditions imposed above. Therefore, for the rigid wall we have to consider the next value of m , which is $m=1$. The corresponding function $\Sigma_R^2(N, \gamma) = -\beta + \sqrt{\beta^2 + \theta/(N+1)}$, where $\beta = (\gamma/2)(2-N)/(N+1)$ is significantly smaller than 1 and smaller than the function $\Sigma_F^2(N, \gamma)$ for the case of the isobaric boundary and the index $m=0$. (The function Σ_F has been shown in Figs. 5 and 7; here we use the indices R and F for the separation of the rigid and soft cases). This must be so since the rigid boundary stabilizes the motion.

As $\gamma \rightarrow \infty$ we have $(\Sigma_R)_m = (-N)/(2m-N) > 0$, $N < 0$. The wave functions of the state $m=1$ are

$$(p_L)_1 = \left(1 - 2\frac{\eta}{N} \right) e^\eta,$$

$$v_1 = (-\eta)^{-N} \left[(\Sigma^{-2} - 1) \left(1 - 2\frac{\eta}{N} \right) + \frac{2}{N} \right] e^\eta.$$

These expressions follow from Eqs. (2.4) and (2.5), $a_1 = -1$, and Eq. (1.6). The function $(p_L)_1(\eta)$ has one zero in the region $\eta < 0$ and it is finite at the rigid boundary. The function $v_1(\eta)$ does not have zeroes inside the region $\eta < 0$. For the factor $(-\eta)^{-N}$, $N < 0$ goes to zero at the boundary $y=0$.

Above we have discussed the asymptotics $k\varepsilon \ll 1$. At the intermediate scales $k \sim 1/\varepsilon$ the increment $\Sigma_R(k)$ transfers to the Brunt-Väisälä asymptote. Therefore the small-scale asymptotes (curve 2 in Fig. 7) for the increments $\Sigma_R(k)$ and $\Sigma_F(k)$ are the same.

VI. INVARIANT POINT AT ACOUSTIC BRANCH

Consider the limit dispersion relation $\sigma^2 = \pm gk$ and the f^\pm modes invariant to the structure of the profile. The spectral problem with the perturbations in an incompressible fluid has the property of hidden symmetry. It is known to have isospectral deformation $\rho_0(y) \rightarrow I\{\rho_0(y)\} = \tilde{\rho}_0(y)$, which keeps the spectrum of eigenvalues unchanged. In contrast to the eigenvalues, the same deformation transforms the eigenfunctions in a nontrivial manner. It is interesting to apply the transformation I to the invariant f^\pm modes since they are not connected, as all other modes, with any definite profile. It is found that the transformation of the f^\pm modes generates modes of the new type. They are also invariant to the stratified profile. The solution with $m=0$, which has been obtained in Sec. V, belongs to this type. In addition, the new fundamental modes are acoustic modes, whereas the isobaric modes are gravity modes. Therefore, below we use the notation f_G^\pm for the isobaric modes and f_P^\pm for the new invariant acoustic modes.

A. Isospectral inversion of density

The inversion of density

$$\rho(\eta) \rightarrow \tilde{\rho}(\eta) = \frac{1}{\rho(-\eta)} \tag{6.1}$$

does not change the eigenvalues. This transformation is nontrivial. It qualitatively changes the profile given by one function $\rho(\eta)$ to another. Existence of this interesting property has been proven firstly for the particular case of three arbitrary sublayers between two homogeneous half-spaces [12]. It has been proven rigorously for the case of an arbitrary number of sublayers in Ref. [24], and for an arbitrary profile

in Ref. [25]. Here we present a very short proof. Its advantage is that it gives the relationship of the duality between conjugate physical functions of Lagrangian pressure p_L and vertical velocity v . This allows us to apply the inversion to the isobaric modes $I\{f_G^\pm\}$.

Inversion (6.1) is isospectral in incompressible fluid. We can extend the results concerning the fundamental modes to the compressible case, since these modes are invariant to the equations of state. To prove isospectrality, we write the equation for p_L [Eq. (1.5)],

$$\left[\frac{d^2}{d\eta^2} - \frac{1}{\rho(\eta)} \frac{d\rho(\eta)}{d\eta} \frac{d}{d\eta} - 1 - \Omega^{-2} \frac{1}{\rho(\eta)} \frac{d\rho(\eta)}{d\eta} \right] p_L(\eta) = 0, \quad (6.2)$$

and add the boundary conditions at infinity $p_L(\pm\infty) = 0$.

We write the equation for v [Eq. (1.5)] in the case of the transformed profile

$$\left[\frac{d^2}{d\eta^2} + \frac{1}{\tilde{\rho}(\eta)} \frac{d\tilde{\rho}(\eta)}{d\eta} \frac{d}{d\eta} - 1 - \Omega^{-2} \frac{1}{\tilde{\rho}(\eta)} \frac{d\tilde{\rho}(\eta)}{d\eta} \right] \tilde{v}(\eta) = 0, \quad (6.3)$$

and add to it the same boundary conditions.

We then calculate the ratio $\tilde{\rho}'(\eta)/\tilde{\rho}(\eta)$ according to rule (6.1), and obtain

$$\frac{\tilde{\rho}'(\eta)}{\tilde{\rho}(\eta)} = \frac{1}{\rho(-\eta)} \frac{d\rho(-\eta)}{d(-\eta)}. \quad (6.4)$$

Substituting Eq. (6.4) into Eq. (6.3), we obtain

$$\left[\frac{d^2}{d(-\eta)^2} + \frac{1}{\rho(-\eta)} \frac{d\rho(-\eta)}{d(-\eta)} \frac{d}{d(-\eta)} - 1 - \Omega^{-2} \frac{1}{\rho(-\eta)} \frac{d\rho(-\eta)}{d(-\eta)} \right] \tilde{v}(\eta) = 0. \quad (6.5a)$$

Defining $\eta = -\xi$ in Eq. (6.5a), we obtain

$$\left[\frac{d^2}{d\xi^2} + \frac{1}{\rho(\xi)} \frac{d\rho(\xi)}{d\xi} \frac{d}{d\xi} - 1 - \Omega^{-2} \frac{1}{\rho(\xi)} \frac{d\rho(\xi)}{d\xi} \right] \tilde{v}(-\xi) = 0. \quad (6.5b)$$

We now compare Eqs. (6.2) and (6.5b). Let the functions $p_L(\eta)$ and $f(\xi) = \tilde{v}(-\xi)$ be solutions of Eqs. (6.2) and (6.5b) with boundary conditions imposed above at the same eigenvalues. We see that the inversion transforms the eigenfunction in the following way:

$$\tilde{v}(-\eta) = p_L(\eta). \quad (6.6a)$$

$$\tilde{p}_L(-\eta) = v(\eta). \quad (6.6b)$$

We see that there are exchanges of the v and p_L functions and changes in the sign of the argument.

In the case of the f_G^\pm modes the pressure perturbations are absent $p_L(\eta) \equiv 0$. Velocities may be found from the first or

second of equations of system (1.1) for $p_L(\eta) \equiv 0$. They are $v^\pm = e^\pm \eta$. Substituting them into the transformation rule (6.6b), we find that

$$(p_L)^\pm(\eta) = e^\mp \eta, \quad \omega^2 = \pm gk. \quad (6.7)$$

Here and below the upper and lower signs correspond to the upper and lower signs in the dispersion relation as it is written in Eq. (6.7). Solutions (6.7) correspond to the f_P^\pm modes. The same solutions may be found from Eq. (1.2) if we substitute in it the relations $\omega^2 = \pm gk$. From this substitution it is easy to see that the functions that define the profile drop out. It appears from this that the distributions p_L , Eq. (6.7), are invariant to the profile structure.

B. Behavior of velocity and boundary conditions

We define the $v^\pm(\eta)$ functions of the f_P^\pm modes. We cannot find them from rule (6.6), so we must return to the system (1.1). At $\omega^2 = \pm gk$, substituting the distributions p_L , Eq. (6.7), into Eq. (1.1), we obtain

$$(v^\pm)'_{\eta^\mp} v^\pm = \left(1 \mp \frac{g}{kc^2} \right) \frac{e^\mp \eta}{\rho}. \quad (6.8)$$

The functions $v^\pm(\eta)$ are found from these equations.

The general solution of Eq. (6.8) depends on two constants C_P and C_G . The first is connected with the function p_L since $(p_L)^\pm = C_P e^\mp \eta$. The second is connected with the first order differential equation (6.8). The general solution of the homogeneous part of Eq. (6.8), $(v^\pm)'_{\eta^\mp} v^\pm = 0$, is $C_G e^\pm \eta$. This means that the general solution of Eq. (6.8) is a mixture of the f_P^\pm and f_G^\pm modes, which are taken with the weights C_P and C_G , respectively.

Above we presented the general description of the f_P^\pm modes. It is interesting to check whether they are compatible with the physical boundary conditions. The isobaric conditions must be omitted since the functions $p_L^\pm = e^\mp \eta$ do not have zeros. Therefore, consider the layer bounded by two rigid walls and find the solutions of Eqs. (6.8) with two zeros.

Consider the case when the right side R of Eq. (6.8) does not change sign. In this case the equation with the lower sign is chosen. Incompressible fluid corresponds to the same case. It can be shown that the solutions are then monotonic functions, and cannot have more than one zero. Therefore, we consider the case of the upper sign. We return to the variable y , with $\eta = ky$, and substitute

$$v^+(y) = e^{ky} w(y).$$

After that we obtain

$$w'_y = k \left(1 - \frac{g}{kc^2} \right) \frac{e^{-2ky}}{\rho} = kR(y). \quad (6.9)$$

We define an arbitrary monotonically increasing or decreasing function $c(y)$ on the interval $y_D < y < y_U$, where y_D and y_U are the lower and upper rigid boundaries, respectively. It is necessary to consider values of k such that the zero of the function $R(y)$, Eq. (6.9), is inside the interval.

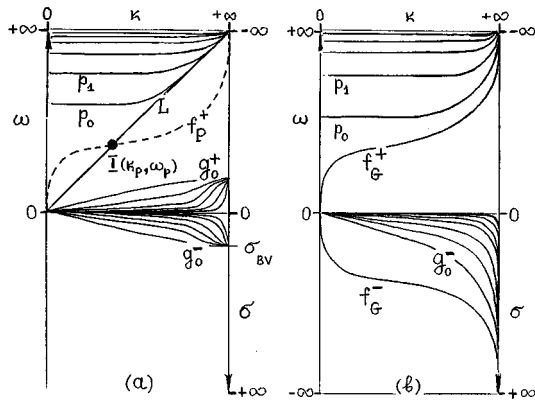


FIG. 8. The spectral sets for the p and g denumerable families of modes. (a) Two rigid boundaries. The point I belongs to the invariant (fundamental) f_P^+ mode. (b) Two isobaric boundaries. The pressure at the upper boundary is $p_V=0$.

Let $R(y_z)=0$ and assume, for definiteness, that the function $c(y)$ decreases with y . Then at $y < y_z$ we have $R(y) > 0$. Integrate Eq. (6.9) from the point $y=y_D$ and let $w(y_D)=0$. Then, for velocity we have $v(y_D)=0$. The solution $w(y)$ of Eq. (6.9) rises within the interval $y_D < y < y_z$. It achieves the maximum at the point $y=y_z$ and after that begins to decrease as y increases.

The variations of k lead to variations in the positions of the point y_z . If we decrease k , the point y_z moves to the lower boundary y_D . If the point y_z is sufficiently close to the lower boundary y_D , the function $w(y)$ after the maximum decreases and reaches zero at the point y_{zz} inside the interval $y_z < y_{zz} < y_U$. It is clear that if we now increase k , the point y_{zz} will move in the upper direction to the upper boundary y_U . Therefore there is a value k_P such that the coincidence $y_{zz}=y_U$ takes place. There is a frequency $\omega_P = \sqrt{gk_P}$ that corresponds to this value of k . At these values of k and ω the function $v(y)$ satisfies both boundary conditions and is therefore the eigenmode of the problem. The point $I(k_P, \omega_P)$ at the k, ω plane corresponds to this mode.

C. Inversion transformation between acoustic and gravity branches

The gas layer bounded by two walls was considered in Sec. VI B. The corresponding spectrum is presented in Fig. 8(a). There are p and g modes. The index m of the acoustic modes p_m , $m=0,1,\dots$ shows the number of zeros of the function $v(y)$ inside the layer. As $k \rightarrow 0$ their frequencies become constants $\approx c/d$, where $d=y_U-y_D$ is the distance between the boundaries and c is some average velocity of sound. As $k \rightarrow \infty$ their frequencies approach the asymptote $\omega = ck$.

There is one more acoustic mode in addition to modes p_m , $m=0,1,\dots$. It has another asymptote as $k \rightarrow 0$. It is marked by label L in Fig. 8(a), and is called the Lamb mode. It is easy to understand its appearance if we consider the limit $g \rightarrow 0$. In this case it is obvious that in the gas layer there is a mode that propagates strictly horizontal. Consider a rectangular box with rigid walls. The acoustic modes are classified by a pair of numbers (m_y, m_x) , where m_y and m_x represent the half wavelengths in the box in the y and x

directions respectively. There are modes $(0,1), (1,0), (1,1), \dots$. The pairs (m_y, m_x) with numbers $m_y=1,2,\dots$ correspond to the modes p_0, p_1, \dots , and all pairs with the number $m_y=0$ correspond to the L mode.

In the homogeneous layer at $g=0$, the velocity v of the L mode is $v(y) \equiv 0$. In the inhomogeneous case, the function $v(y)$ is defined by the inhomogeneity. It does not have zeros inside the profile in the case of the monotonic profile and it has one or more zeros in the case of nonmonotonic profiles. The L mode is eliminated if one or two boundaries are isobaric; see, e.g., Fig. 8(b). It is important that at the fixed boundary conditions the qualitative structure of the acoustic L and p_m modes is conserved at $g \neq 0$.

At $g \neq 0$ the gravity modes g_m^\pm appear. Here, $m=0,1,\dots$ gives the number of zeros of the function $v(y)$. In the limit of shallow water $k \rightarrow 0$ or the long-wavelength limit their frequencies are

$$\omega_m = \xi_m \sqrt{(d \ln s/dy) d} ck = \alpha \xi_m \sqrt{(d \ln s/dy) d} \sqrt{ghk},$$

where $h=c^2/g$, $d=y_U-y_D$, the numbers ξ_m, α depend on the profile structure, and $\xi_m \rightarrow 0$ as $m \rightarrow \infty$.

The point I from the invariant mode f_P^+ is the intersection point of the dispersion curve of the L mode and the curve $\omega = \sqrt{gk}$. Its coordinates are k_P and ω_P (see Sec. VI B).

The full spectrum of the polytrope bounded by the two isobaric boundaries studied here is presented in Fig. 8(b) for comparison. There are $p_m, f_G^+, g_m^-,$ and f_G^- modes. Index m gives the number of zeros of function $p_L(y)$. The modes f_G^+ and g_m^- are connected with the upper boundary y_V and the mode f_G^- with the lower boundary y_A .

As stated above, the different eigenfunctions correspond to the f_P^\pm and f_G^\pm modes. The first have the exponential pressures p_L and the second have exponential velocities v . We see that the acoustic and gravity families are symmetric now, with both having their own invariant (fundamental) modes that separate them.

VII. THERMODYNAMICS OF SUBSHELLS

The work is dedicated to the study of the spectral properties of the inverse density polytropes. The results are used for the simulation of the linear stage of the development of the RT instability in the multilayer targets. Is this approach adequate to the real situation? The targets consist of a large number of subshells made from different materials. Is it possible to describe the process of the development by one polytrope when (a) the EOS of the materials are nonideal, and (b) these EOS are different in the different subshells?

We now answer these questions. The targets with the power-law distribution of density ρ are fabricated by selecting the chain of substances of increasing densities $\rho_J < \rho_{J-1} < \dots < \rho_1$ and adjusting the thicknesses of the subshells. It is assumed that the multilayer target is in the effective gravity field. This is the standard approximation used by many authors. Then the hydrostatic equation is valid: $p'_y = -g\rho$. It appears from this that, if we neglect the pressure p_V in the cavity, then the pressure profile will be the power-law profile. The difference between the power-law indices for the pressure and density distributions equals 1.

Therefore, the ratio p/ρ is the linear function of the coordinate.

The model is based on the dynamic equation (1.2), which is valid at arbitrary EOS. The inertial and thermodynamic conditions must be fulfilled to go from Eq. (1.2) to the solutions presented in Secs. II and III. The inertial conditions (the power-law profile of ρ , the linear dependence of p/ρ) are fulfilled. We now consider the thermodynamic condition. It is the condition for the linear dependence of the function c^2 on the coordinate.

Consider this condition. Write the thermodynamic relation between the functions c^2 and p/ρ . From the definitions of c^2 and γ_R , we have

$$c^2 = \gamma_R \frac{p}{\rho}, \quad c^2 = \left(\frac{\partial p}{\partial \rho} \right)_S, \quad \gamma_R = \left(\frac{\partial \ln p}{\partial \ln \rho} \right)_S. \quad (7.1)$$

In the case of nonideal EOS, the index γ_R in the adiabatic processes is the function of one thermodynamic variable, e.g., density $\gamma_R = \gamma_R(\rho)$. In different subshells this function will be different $\gamma_R^j(\rho)$, where the index j enumerates the subshells. Here we consider the hydrostatic or steady-state distributions. In the steady state the densities of the subshells are fixed as ρ_j . Therefore, the thermodynamic indices depend on the index of the subshell only $\gamma_R^j(\rho) = \gamma_R^j(\rho_j) = \gamma_R^j$. The ratio p/ρ in Eq. (7.1) is linear. For applicability of our approach, the indices γ_R^j must therefore be the same in different subshells.

From numerous studies of EOS it is known that the indices γ_R differ moderately for different substances. The influence of these variations on our results is not significant. The main result is the partial stabilization of the RT instability as shown in Fig. 5. This is the reduction of the increment σ due to the shift R . The conclusion about the reduction remain true if the indices γ_R are different in different subshells. This

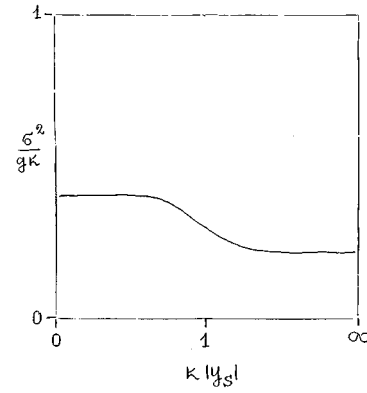


FIG. 9. The smooth transformation of the increment in the two-layer case.

means that the inertial conditions are more significant for the dynamics of the instability than the thermodynamic one.

We use a two-layer example to show this. Let the index be $\gamma = \gamma_U$ at $y_S < y < 0$ and $\gamma = \gamma_D$ at $y < y_S$. In this case the increment σ is defined by the index γ_U at large wave numbers $k|y_S| \gg 1$ and by the index γ_D at small wave numbers $k|y_S| \ll 1$. The monotonic transformation of the increment takes place in the crossover region $k|y_S| \sim 1$ as shown in Fig. 9. This is because the small-scale perturbations are located in the upper sublayer and, on the other hand, this sublayer is unessential for the large-scale perturbations.

It appears from this that the increment remains inside the dashed strip in Fig. 5 for all wavelengths in the problem with variable index γ_R . Therefore, the increment also remains reduced in this problem.

ACKNOWLEDGMENT

The work was sponsored by the Russian Basic Research Foundation (RBRF) under Grant No. 95-02-06381-a.

-
- [1] J. H. Nuckolls, L. Wood, A. R. Thiessen, and G. B. Zimmerman, *Nature (London)* **239**, 139 (1972).
 - [2] K. A. Brueckner and S. Jorna, *Rev. Mod. Phys.* **46**, 325 (1974).
 - [3] J. D. Lindl, R. L. McCrory, and E. M. Campbell, *Phys. Today* **45**, 32 (1992).
 - [4] S. W. Haan, S. M. Pollaine, J. D. Lindl, L. J. Suter, R. L. Berger *et al.*, *Phys. Plasmas* **2**, 2480 (1995).
 - [5] R. McEachern, C. Moore, G. E. Overturf, III, S. R. Buckley, and R. Cook, *ICF Q. Rep. LLNL* **4**, 25 (1993).
 - [6] S. A. Letts, G. W. Collins, E. M. Fearon *et al.*, *ICF Q. Rep. LLNL* **4**, 54 (1994).
 - [7] S. W. Haan, P. A. Amendt, G. L. Strobel, D. B. Harris, S. M. Pollaine *et al.*, *ICF Q. Rep. LLNL* **5**, 215 (1995).
 - [8] O. L. Landen, N. D. Hoffman, M. D. Cable, H. N. Kornblum, C. J. Keane *et al.*, *ICF Q. Rep. LLNL* **5**, 271 (1995).
 - [9] J. Glimm and D. H. Sharp, *Phys. Rev. Lett.* **64**, 2137 (1990).
 - [10] D. Shvarts, U. Alon, D. Ofer, C. P. Verdon, and R. L. McCrory, *Phys. Plasmas* **2**, 2465 (1995).
 - [11] N. A. Inogamov, *Dokl. Akad. Nauk SSSR* **278**, 57 (1984) [*Sov. Phys. Dokl.* **29**, 714 (1984)].
 - [12] K. O. Mikaelian, *Phys. Rev. A* **26**, 2140 (1982).
 - [13] C. Cherfilis and K. O. Mikaelian, *Phys. Fluids* **8**, 522 (1996).
 - [14] H. Takabe, K. Mima, L. Montierth, and R. L. Morse, *Phys. Fluids* **28**, 3676 (1985).
 - [15] M. H. Emery, J. H. Gardner, and S. E. Bodner, *Phys. Rev. Lett.* **57**, 703 (1986).
 - [16] G. Dimonte, C. E. Frerking, and M. Schneider, *Phys. Rev. Lett.* **74**, 4855 (1995).
 - [17] W. Unno, Y. Osaki, H. Ando, and H. Shibahashi, *Nonradial Oscillations of Stars* (University of Tokyo Press, Tokyo, 1979).
 - [18] J. P. Cox, *Theory of Stellar Pulsation* (Princeton University Press, Princeton, 1980).
 - [19] H. Lamb, *Hydrodynamics* (Dover, New York, 1945), Chap. X.
 - [20] C. L. Pekeris, *Phys. Rev.* **73**, 145 (1948).
 - [21] A. Skumanich, *Astrophys. J.* **121**, 408 (1955).
 - [22] J. Christensen-Dalsgaard, D. O. Gough, and J. Toomre, *Science* **229**, 923 (1985).

- [23] L. J. Slater, in *Handbook of Mathematical Functions*, edited by M. Abramowitz and I. A. Stegun, NBS Applied Math Series No. 55 (GPO, Washington, DC, 1964).
- [24] N. A. Inogamov, in *Problems of Dynamics and Stability of Plasma*, (Moscow Institute for Physics and Technology, Moscow, 1990), p. 100 (in Russian).
- [25] H. J. Kull, *Phys. Rep.* **206**, 197 (1991).